Heliyon 9 (2023) e19878

Contents lists available at ScienceDirect

Heliyon

journal homepage: www.cell.com/heliyon

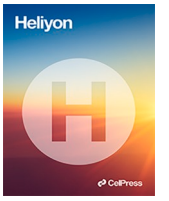

Mir-142-5p inhibits the osteogenic differentiation of bone marrow mesenchymal stem cells by targeting Lhx8

Yongjun Du [a,b,1], Hui Zhong [a,1], Chen Yu [a], Yan Lv [a,c], Yueyi Yao [d], Zhi Peng [a,*], Sheng Lu [a,**]

[a] Orthopaedics Department, The First People's Hospital of Yunnan Province, The Affiliated Hospital of Kunming University of Science and Technology, The Key Laboratory of Digital Orthopaedics of Yunnan Provincial, Yunnan Provincial Center for Clinical Medicine in Spinal and Spinal Cord Disorders, Kunming, 650034, China

[b] Medical School, Kunming University of Science and Technology, Kunming, Yunnan 650500, China

[c] Faculty of Life science and Technology, Kunming University of Science and Technology, Kunming, 650500, China

[d] Science and Technology Achievement Incubation Center, Kunming Medical University, 1168 Chunrongxi Road, Kunming, Yunnan 650500, China

ARTICLE INFO

Keywords:
Osteoporosis
Lhx8
Osteogenic differentiation
miR-142-5p
Bone marrow mesenchymal stem cells

ABSTRACT

Osteoporosis (OP), a common systemic bone metabolism disease with a high incidence rate, is a serious health risk factor. Osteogenic differentiation balance is regulated by bone marrow mesenchymal stem cells (BMSCs) and plays a key role in OP occurrence and progression. Although, LIM homeobox 8 (Lhx8) has been identified to affect BMSCs osteogenic differentiation, its roles in OP and the associated mechanism remains unclear. Here, we aimed to elucidate the role and mechanism of Lhx8 in the osteogenic differentiation of BMSCs. BMSCs isolated from wild type and OP Sprague–Dawley rats were cultured and confirmed via flow cytometry and microscopy. Based on dual-luciferase reporter assay, BMSCs were transfected with miR-142-5p mimics and miR-NC (negative control). Real-time quantitative reverse transcription polymerase chain reaction and Western blot analyses were performed to determine the role of Lhx8 in BMSCs osteogenic differentiation. Lhx8 expression was significantly reduced in OP, whereas that of miR-142-5p, a possible Lhx8 regulator, was significantly upregulated. Dual-luciferase reporter assay demonstrated that miR-142-5p exerted a direct targeted regulatory effect on Lhx8. Moreover, miR-142-5p mimics significantly inhibited BMSCs osteogenic differentiation as well as Lhx8 expression in vitro, indicating that miR-142-5p may be involved in BMSCs osteogenic differentiation via Lhx8 expression regulation and may serve as a potential diagnostic target for OP. Overall, these findings indicated that miR-142-5p inhibits BMSCs osteogenic differentiation by suppressing Lhx8. These may serve as a foundation for further studies on OP treatment based on miR-142-5p targeting.

1. Introduction

In 1993, the World Health Organisation defined osteoporosis (OP) as a systemic skeletal disease [1] characterised by a low bone

* Corresponding author.
** Corresponding author.
E-mail addresses: zhiandpeng@126.com (Z. Peng), drlusheng@163.com (S. Lu).
[1] Co-first authors, contributed equally to this work.

https://doi.org/10.1016/j.heliyon.2023.e19878
Received 21 May 2023; Received in revised form 31 August 2023; Accepted 4 September 2023
Available online 9 September 2023

mass and microarchitectural deterioration of bone tissue, which lead to increased bone fragility and susceptibility to fractures. OP severely affects the health and quality of life of patients and may even be life-threatening [2,3]. Bone marrow mesenchymal stem cells (BMSCs) are stem cells that are capable of self-renewal and multilineage differentiation into osteoblasts, chondrocytes, and adipocytes under different conditions [4–6]. Additionally, osteogenic differentiation of BMSCs plays an important role in maintaining osteocyte number and the dynamic balance between bone formation and resorption [7–9]. However, a weakening of the osteogenic differentiation ability of BMSCs leads to an imbalance of bone homeostasis, with bone resorption exceeding bone formation, which is the primary cause of diseases such as OP and non-healing bone fractures [10–14]. Therefore, enhancing the osteogenic differentiation ability of BMSCs is critical in the treatment of OP and related diseases.

LIM homeobox 8 (Lhx8), a member of the LIM homeobox family, is a transcription factor that is highly conserved across species. Previous studies have shown that LHX8/SUV39HL is highly expressed during the early stages of dental development. However, the expression level decreases during later stages to achieve a balance between dental mesenchyme differentiation and proliferation [15,16]. It has also been reported that LHX8 overexpression promotes the proliferation of human dental pulp stem cells, inhibit odontogenic differentiation, and negatively regulates the differentiation and maturation of mesenchymal tissue [16,17]. This finding suggests that LHX8 possibly plays an important role in regulating the balance between MSC proliferation and differentiation. Additionally, LHX8 can significantly promote BMSC proliferation [18] and regulate BMSCs osteogenic differentiation [19]. However, the exact regulatory mechanism of LHX8 yet to be elucidated. Therefore, investigating the functional mechanism of LHX8 in osteogenic differentiation via a sequencing approach would enhance the understanding of bone regeneration.

MicroRNAs (miRNAs), small non-coding RNA molecules that are 18–25 nucleotides long, can regulate gene expression at the post-transcriptional level [20]. Specifically, miRNAs can bind to complementary sequences in target mRNAs and inhibit target mRNA expression via post-transcriptional regulation, thereby forming a complex regulatory network [21,22]. Further, miRNAs can regulate the majority of biological processes, including cell growth, development, differentiation, proliferation, metabolism, and cell cycle [23]. Moreover, miRNAs also play important roles in bone formation and resorption [24] by regulating the differentiation of BMSCs. Therefore, an analysis of the regulatory relationships between miRNAs and LHX8 at the transcriptomic level can provide novel possibilities for the diagnosis, prevention, and treatment of OP.

2. Materials and methods

2.1. Ovariectomised (OVX) animal model

Six-week-old specific pathogen-free (SPF) female Sprague–Dawley (SD) rats purchased from Kunming Medical University (Yunnan, China) were used as the experimental animals. All the animal experiments were performed in strict accordance with the Guidelines for the Care and Use of Laboratory Animals and were approved by the Animal Care and Use Committee of Kunming Medical University. To establish the OVX model, the rats were anaesthetised and their ovaries were sufficiently exposed via dorso-lateral incisions. Subsequently, their fallopian tubes and the adjacent blood vessels were ligated, and their ovaries were removed. Rats in the sham group were only subjected to skin and muscle incision followed by suturing. After surgery, each rat was placed on a platform maintained at 37 °C until they regained consciousness. Symptoms of OP were confirmed postoperatively in the OVX model rats at 3 months.

2.2. Isolation, culturing, and identification of BMSCs

BMSCs were isolated from the femur and tibia of SD rats using the whole bone marrow adherence method. Briefly, femur and tibia collected from the lower limbs of the rats were cut open at the ends to expose the bone marrow cavity. Subsequently, the bone marrow cavity was repeatedly washed with an α-minimum essential medium (α-MEM) (Gibco, Grand Island, USA) containing 1% penicillin/streptomycin (Gibco). The cell-containing wash solution was collected and centrifuged. The supernatant was discarded, and the cells were uniformly mixed in an α-MEM culture medium containing 10% foetal bovine serum (FBS; Gibco, Melborne, Australia) and 1% penicillin/streptomycin; the resulting medium was transferred to a T25 culture flask, and cultured in a 5% CO_2 incubator at 37 °C. The culture medium was replaced every two days and cell passaging was performed when the cells reached 80%–90% confluence. To identify BMSCs, the cells were incubated with anti-CD90, -CD45, -CD29, and -CD44 antibodies (eBioscience™/Invitrogen, Waltham, USA) at room temperature for 30 min. Thereafter, surface markers for BMSCs were measured via flow cytometry, and cell morphology was determined using a phase contrast microscope. Flow cytometry was repeated three times using samples obtained from three SD rats.

2.3. miRNA sequencing (miRNA-Seq) analysis of BMSCs

Total RNA was isolated from BMSCs (four samples per group) using Trizol reagent (Invitrogen, Waltham, USA). The quality and quantity of RNA were assessed using Agilent 2100 (Agilent Technologies, Amstelveen, the Netherlands) and Nanodrop 2000 (Thermo., Wilmington, USA), respectively. Sequencing libraries were prepared from total RNA using the TruseqTM Small RNA sample prep Kit (Illumina, California, USA). High throughput sequencing was performed using NovaSeq 6000 (Illumina, San Diego, USA). Adapter and low-quality reads (<Q20) were removed using Fastp (https://github.com/OpenGene/fastp), which was followed by the mapping of clean data (reads) to the reference genome using Bowtie (http://bowtie-bio.sourceforge.net/index.shtml). Gene expression levels were estimated using miRDeep2 (https://www.mdc-berlin.de/content/mirdeep2-documentation), and the normalized values were expressed as TPM (Transcripts Per Millon). Subsequently, a differential expression analysis was performed using DESeq2 (http://

bioconductor.org/packages/stats/bioc/DESeq2/).

2.4. Osteogenic differentiation and alizarin red staining

BMSCs from passage 3 (P3) at ≥80% confluence, were digested and used to prepare a single-cell suspension, which was then seeded in a 6-well plate containing gelatine at a density of 2×10^5 cells/well. Subsequently, the growth medium (2 mL) was added to each well, and the 6-well plate was cultured in a 5% CO_2 incubator at 37 °C. At ≥70% confluence, the growth medium was replaced with osteogenic differentiation medium (OriCell®, Guangzhou, China), which was changed at 3-day intervals. After 4 weeks of differentiation induction, the cells were stained with alizarin red, according to instructions provided with the OriCell® kit. In brief, the cells were fixed in 4% paraformaldehyde solution at room temperature for 30 min, washed gently with PBS, and stained with the alizarin red working solution. After the excess dye was washed away with PBS, the stained cells were observed and photographed under an inverted microscope. The BMSCs differentiation induction experiment was repeated three times for each group.

2.5. Dual-luciferase reporter assay

The hypothetical binding site of miR-142-5p on Lhx8 was predicted using TargetScan (https://www.targetscan.org/vert_71/). The 3'-untranslated regions (3′-UTRs) of wild-type and mutant Lhx8 containing the hypothetical target site for miR-142-5p were amplified and cloned into the pmirGLO vector (Promega, Madison, USA), which was subsequently co-transfected with miR-142-5p mimics or miR-NC into 293T cells using Lipofectamine 2000 (Invitrogen, Carlsbad, USA). After 48 h of transfection, luciferase activity was measured using the dual-luciferase reporter assay system (Promega).

2.6. Cell transfection

miR-142-5p mimics (5′-CAUAAGUAGAAAGCACUACU-3′) and its negative control, miR-NC, were obtained from Genechem (Shanghai, China). Firstly, BMSCs were inoculated into a 6-well plate at a density of 2×10^5 cells per well. At 70% confluence, the cells were transfected with miR-142-5p mimics or miR-NC using Lipofectamine 3000 (Invitrogen, Carlsbad, USA). The transfected cells were further cultured for 48 h and subsequently subjected to real-time quantitative reverse transcription polymerase chain reaction (qRT-PCR) to measure the transfection rate.

2.7. qRT-PCR

Total RNA was extracted from BMSCs (four samples per group), using TRIzol reagent (Invitrogen, Carlsbad, USA) and the reverse-transcribed using the PrimeScript™ RT-PCR kit/Mir-X miRNA First-Strand Synthesis Kit (Takara Bio, Dalian, China). RNA sample used to determine the miR-142-5p expression was reverse-transcribed by adding ploy (A) tail, which was followed by performing qRT-PCR using reverse universal primers from the Mir-X miRNA First-Strand Synthesis Kit and forward specific primers containing the complete sequence of the mature miR-142-5p. qRT-PCR was then performed using the TB Green® kit (Takara Bio, Dalian, China), mRNA and miR-142-5p expression levels were quantified using the $2^{-\Delta\Delta CT}$ method, with GAPDH and U6 being the housekeeping genes for normalisation. The primer information is shown in Table S1.

2.8. Western blotting

Total protein was extracted from BMSCs using RIPA and PMSF (Solarbio, Beijing, China), and then quantified using the BCA protein assay kit (Beyotime, Shanghai, China). Thereafter, 10 μg of the protein sample was separated via sodium dodecyl sulphate-polyacrylamide gel electrophoresis (SDS-PAGE) using 10% SDS-PAGE gel and transferred onto a polyvinylidene fluoride (PVDF) membrane (Bio-Rad, Hercules, CA, USA). After non-specific blocking, the membrane was incubated with specific primary antibodies (LHX8, Abcam, Cambridge, UK; glyceraldehyde 3-phosphate dehydrogenase [GAPDH], osteocalcin [OCN], osteopontin [OPN], all Proteintech, Chicago, USA) overnight at 4 °C. The membrane was then incubated with the corresponding secondary antibodies at room temperature for 2 h. Finally, the protein blot was quantified using an enhanced chemiluminescence (ECL) kit (Millipore, Billerica, USA) and imaged using a Bio-Rad imaging system. Western blotting was performed with three replicates.

2.9. Statistical analysis

Statistical analyses were performed using SPSS software version 25.0 (IBM, Armonk, NY, USA). Significant differences between more than two groups were determined using one-way ANOVA. All data were expressed as mean ± standard deviation (SD, $n \geq 3$), and means were considered statistically significant at $p < 0.05$ ($^*p < 0.05$, $^{**}p < 0.01$, $^{***}p < 0.001$).

3. Results

3.1. Lhx8 expression level increased during BMSC osteogenic differentiation

BMSCs isolated from the femur of SD rats and cultured to P3 exhibited a spindle-shaped morphology based on observation under a

microscope (Fig. S1a). To confirm the quality of the BMSCs, the expression of the specific surface marker of P1 cells were determined using flow cytometry. $CD29^{+}$, $CD44^{+}$, $CD45^{-}$, and $CD90^{+}$ cells accounted for more than 90% of the cell population (Fig. 1), which is consistent with the definition of MSCs [25]. Additionally, P3 BMSCs possessed the ability to differentiate into the osteogenic, adipogenic, and chondrogenic lineages, confirming the multilineage potential of the cells (Fig. S1).

To determine the role of LHX8 in BMSCs, we investigated its protein and mRNA expression levels during BMSC differentiation. There was an increase in the expression of the osteogenic differentiation markers, OCN, OPN, and runt-related transcription factor 2 (Runx2) following the induction of BMSCs osteogenic differentiation (Fig. 2a and b, Fig. S4). Alizarin red staining showed an increase in calcium nodules (Fig. S2), confirming effective differentiation into osteoblasts. Additionally, Lhx8 expression was significantly upregulated at both the protein and mRNA expression levels (Fig. 2c and d, Fig. S5). These dynamic changes in Lhx8 expression level suggested that Lhx8 possibly plays a promotive role in the osteogenic differentiation of BMSCs.

3.2. *Lhx8 was under expressed in OP rats*

Ovariectomy was performed in SD rats to establish an OVX model to further investigated the expression and mechanism of action of Lhx8 in rats with OP. Micro computed tomography (Micro-CT) analysis showed a significant decrease in bone mineral density (BMD), trabecular number, and trabecular thickness, and a significant increase in trabecular separation in rats in the OVX model group when compared with those of rats in the sham group (Fig. 3a). These results confirmed that an SD rat model with a lower BMD was established successfully. Further, BMSCs were extracted from rats in the OVX model and sham groups for validation via qRT-PCR and Western blotting analysis. Compared with that of the sham group, Lhx8 expression was significantly downregulated in the OVX model group at both the mRNA and protein expression levels (Fig. 3b–e, Fig. S6), indicating that Lhx8 may be involved in OP regulation.

3.3. *miR-142-5p was overexpressed in OP rats*

TargetScan (https://www.targetscan.org/vert_80/) was used to predict miRNAs that may participate in the regulation of Lhx8. The prediction revealed the possible existence of interactions between 20 miRNAs and Lhx8 (Table S2). RNA sequencing was performed to further confirm miRNAs involved in Lhx8 regulation, and a total of 379 miRNAs were identified. Differential expression analysis (Based on $|\log 2$ fold change (FC)$| > 2$ and p.adjust <0.05), identified 17 significantly upregulated and seven downregulated miRNAs

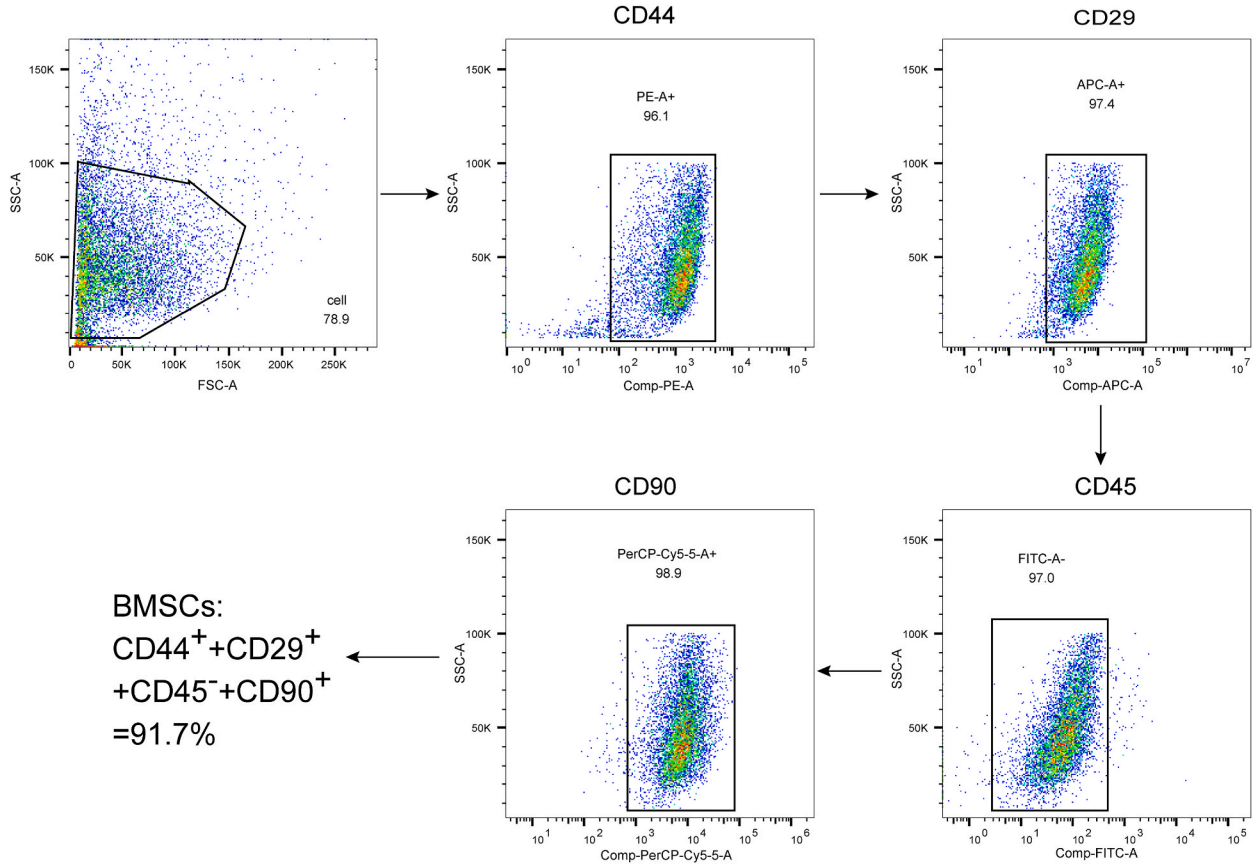

Fig. 1. Identification of BMSCs by flow cytometry.

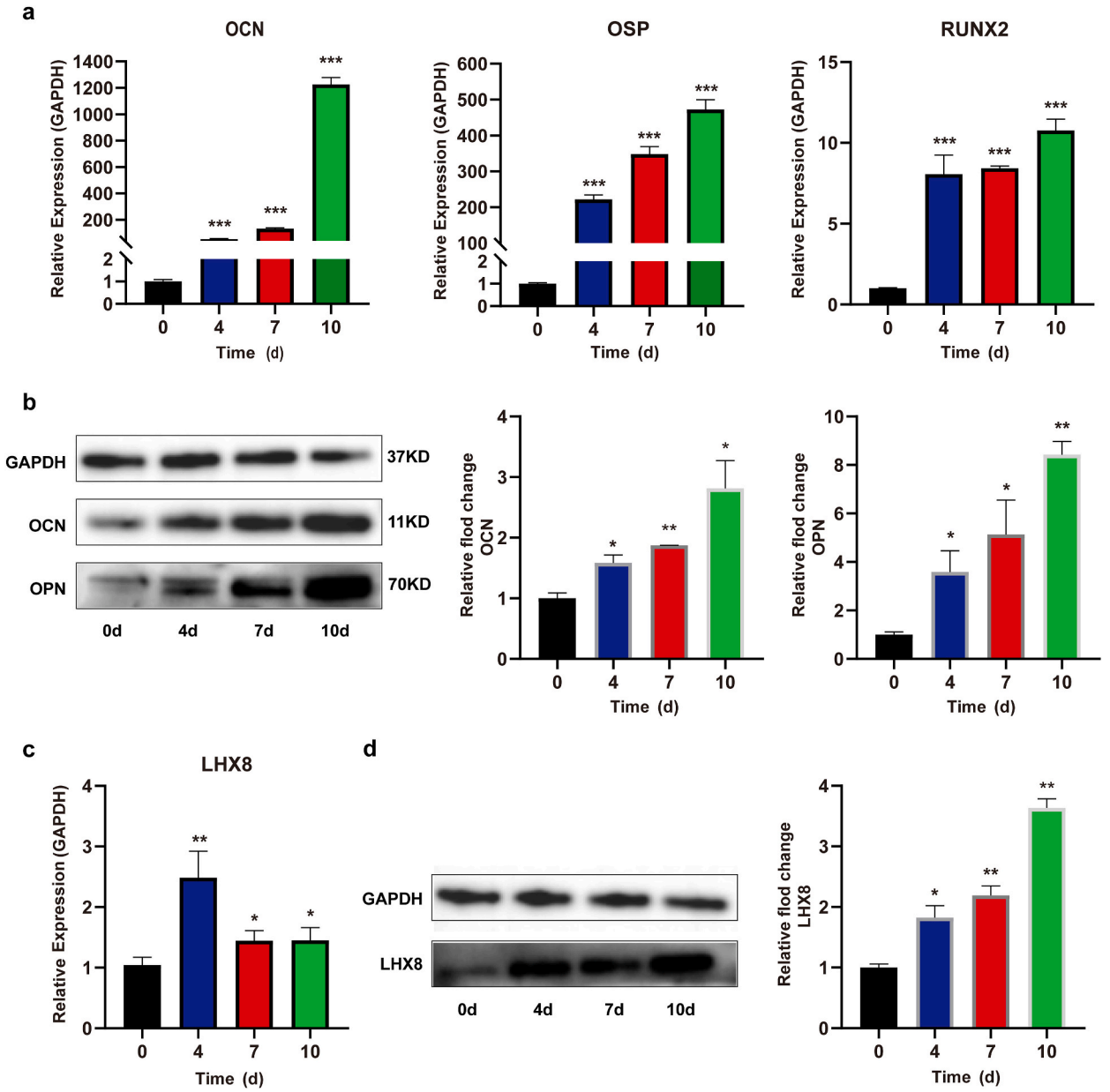

Fig. 2. Lhx8 was significantly upregulated during osteogenic differentiation. a. Osteogenic marker genes were upregulated during osteogenic differentiation; b. Osteogenic marker proteins were upregulated during osteogenic differentiation; c. *Lhx8* expression was upregulated during osteogenic differentiation; d. Lhx8 protein expression was upregulated during osteogenic differentiation. $*p < 0.05$, $**p < 0.01$, $***p < 0.001$.

(Fig. 4a, Table 1). Venn diagram analysis also showed that miR-142-5p (log 2 FC = 3.660232683) and miR-384-5p (log 2 FC = 2.429335129) were located in the intersection between the upregulated and predicted miRNAs (Fig. 4b). However, when we predicted the target genes of miR-142-5p and miR-384-5p using TargetScan, Lhx8 was only present in the set of target genes predicted for miR-142-5p. Moreover, RT-PCR showed an increase in miR-142-5p expression in the BMSCs of rat in the OVX model group compared with sham group rats (Fig. 4c). This suggested that miR-142-5p may participate in OP pathogenesis in rats by silencing Lhx8 and reducing its protein expression.

3.4. Inhibition of BMSC osteogenic differentiation via mir-142-5p upregulation was associated with Lhx8

The mature sequences of miR-142-5p in humans and SD rats are identical (Fig. 5a). According to predictions based on TargetScan (https://www.targetscan.org/vert_80/), miR-142-5p has complementary binding sites on the 3'-UTR region of Lhx8. Additionally, the seed region sequence (439–446 nt) was found to be identical across species (Fig. 5a). Moreover, dual-luciferase reporter assay showed

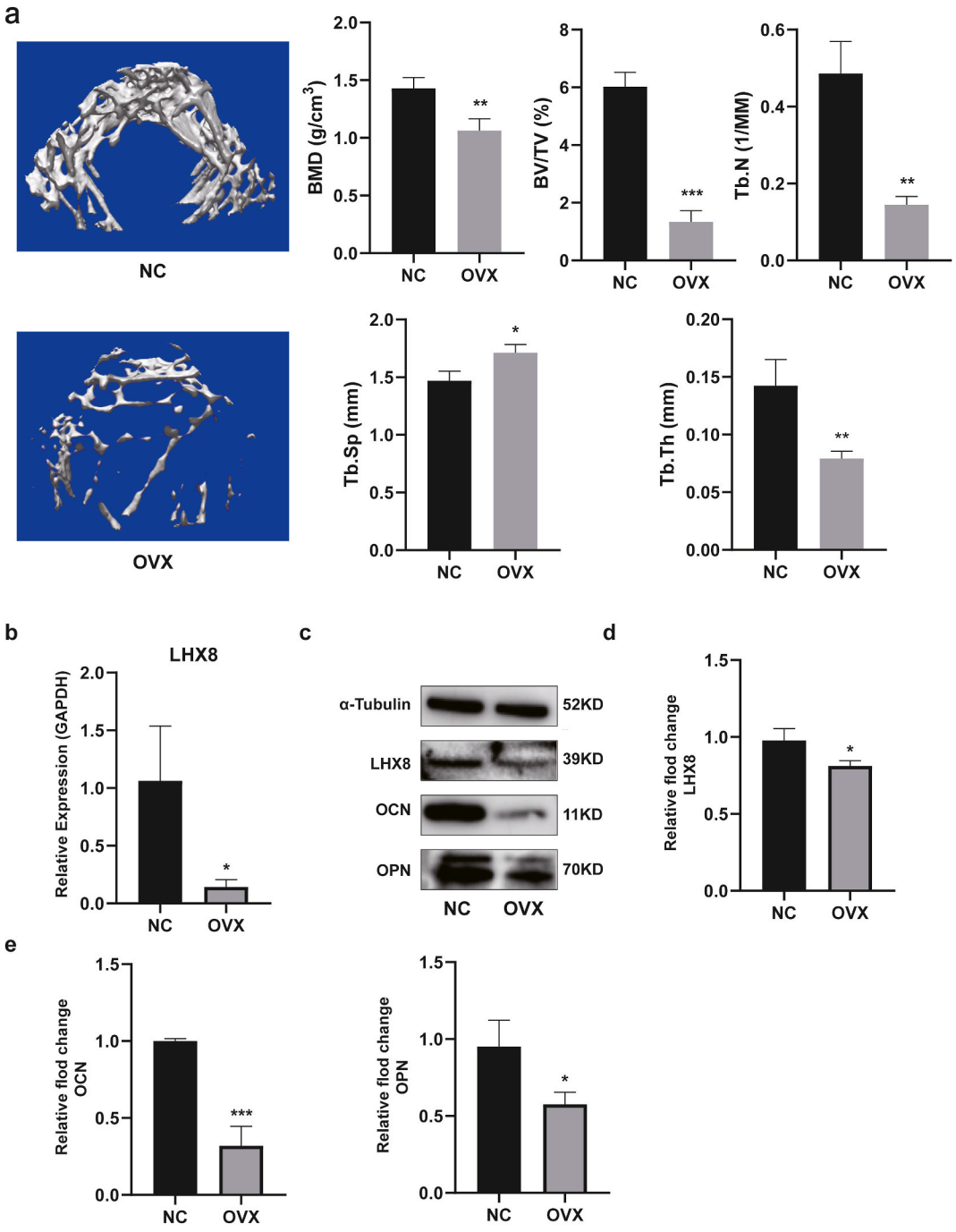

Fig. 3. Lhx8 was significantly downregulated in osteoporosis. a. Micro-CT three-dimensional reconstruction of cancellous bone and bone mineral density. Statistical analysis of bone volume fraction, bone trabecular number, bone trabecular separation, and bone trabecular thickness between OVX model and sham groups; b. *Lhx8* gene expression was downregulated in the OVX group; c. Lhx8 protein expression in the OVX group; d. Statistics of Lhx8 protein expression level in OVX group; e. Statistics of protein expression levels of the osteogenic markers OCN and OPN in OVX group. $^{*}p < 0.05$, $^{**}p < 0.01$, $^{***}p < 0.001$.

that pmirGLO-LHX8-WT showed reduced luciferase activity in the presence of miR-142-5p mimics, whereas pmirGLO-LHX8-MT luciferase activity was not significantly affected (Fig. 5b). Overall, these results suggest that miR-142-5p could directly target LHX8.

To elucidate the function of miR-142-5p in BMSCs, BMSCs were transfected with miR-142-5p mimics. The results of qRT-PCR showed that miR-142-5p transfection significantly increased miR-142-5p expression in BMSCs (Fig. 6a), and it significantly decreased Lhx8 expression at both the mRNA (Fig. 6b) and protein (Fig. 6c, Fig. S7) expression levels. Subsequently, osteogenic

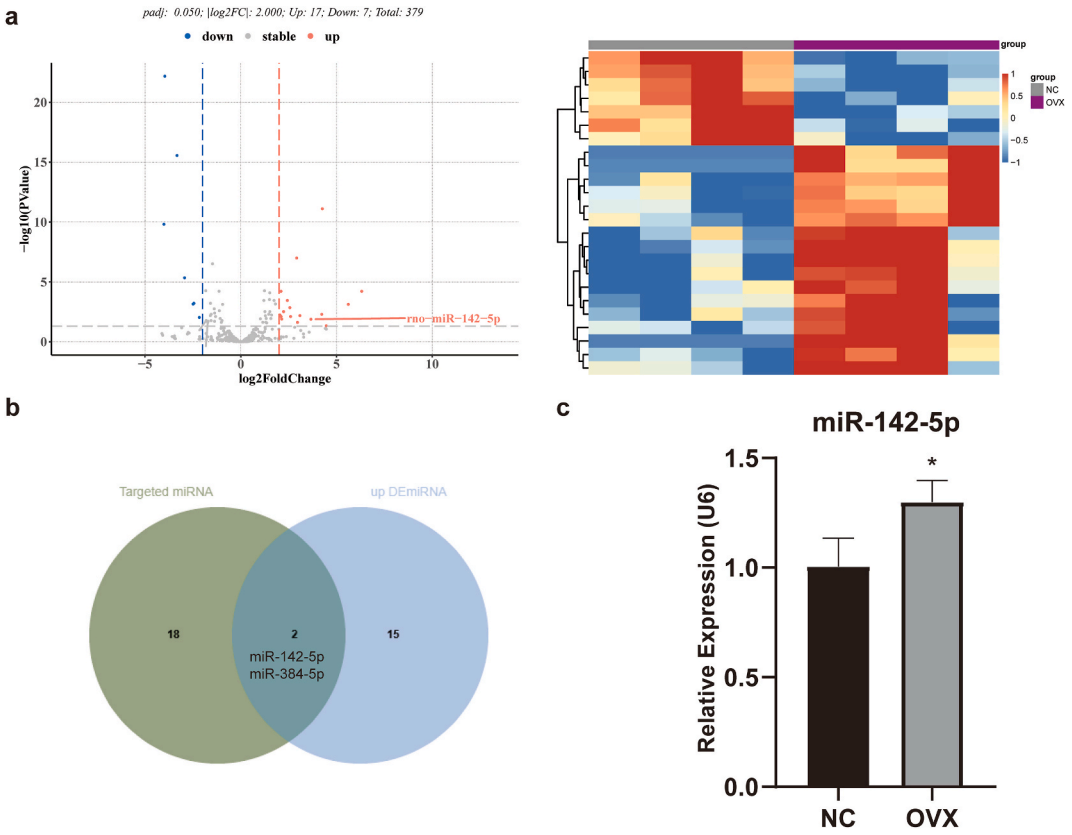

Fig. 4. miR-142-5p was significantly upregulated in osteoporosis. a. Volcano and heat maps of differentially expressed miRNAs in OVX group; b. Predicted miRNAs and upregulated miRNAs were shown in a Venn diagram; c. miR-142-5p expression level in OVX group.

Table 1
The differentially expressed miRNAs.

miRNA	baseMean	log2FC	lfcSE	stat	pvalue	padj	change
miR-335	283.3532	−3.96723	0.380253	−10.4332	1.75E-25	6.63E-23	down
miR-708-5p	247.2558	−3.33066	0.37887	−8.79102	1.48E-18	2.81E-16	down
miR-223-3p	1104.406	4.26201	0.567937	7.504369	6.17E-14	7.80E-12	up
miR-708-3p	143.7301	−4.01525	0.568384	−7.06433	1.61E-12	1.53E-10	down
miR-10a-5p	716.5323	2.915636	0.480836	6.063677	1.33E-09	1.01E-07	up
miR-129-5p	204.4202	−2.93848	0.548263	−5.35962	8.34E-08	4.52E-06	down
miR-10b-5p	471.2524	2.09806	0.440339	4.764646	1.89E-06	5.98E-05	up
miR-511-5p	7.736639	6.31687	1.322598	4.776107	1.79E-06	5.98E-05	up
miR-384-5p	101.0051	2.429335	0.561649	4.325365	1.52E-05	0.000352	up
miR-452-3p	31.95506	−2.45087	0.587602	−4.17096	3.03E-05	0.000605	down
miR-130b-3p	34.08948	−2.48996	0.605037	−4.11539	3.87E-05	0.000698	down
miR-429	4.734025	5.616327	1.373344	4.089526	4.32E-05	0.000745	up
miR-325-3p	36.53897	2.559276	0.652697	3.921075	8.82E-05	0.001392	up
miR-211-5p	152.0391	2.233395	0.604575	3.694155	0.000221	0.002986	up
miR-10a-3p	8.71767	4.231429	1.204105	3.514169	0.000441	0.005066	up
miR-101a-3p	2374.096	2.043625	0.588412	3.473119	0.000514	0.005735	up
miR-223-5p	26.19742	3.085731	0.90157	3.422619	0.00062	0.006504	up
miR-338-3p	18.66568	2.100608	0.626796	3.35134	0.000804	0.007815	up
miR-146a-3p	68.31875	2.59795	0.776849	3.344214	0.000825	0.007818	up
miR-92b-3p	12.23012	−2.16478	0.659385	−3.28303	0.001027	0.009267	down
miR-146a-5p	3551.771	2.136075	0.675723	3.161169	0.001571	0.012671	up
miR-142-5p	145.1554	3.660233	1.163891	3.144825	0.001662	0.013122	up
miR-511-3p	13.14625	2.958101	1.01804	2.905681	0.003665	0.024192	up
miR-501-5p	2.129507	4.465167	1.665707	2.680644	0.007348	0.046415	up

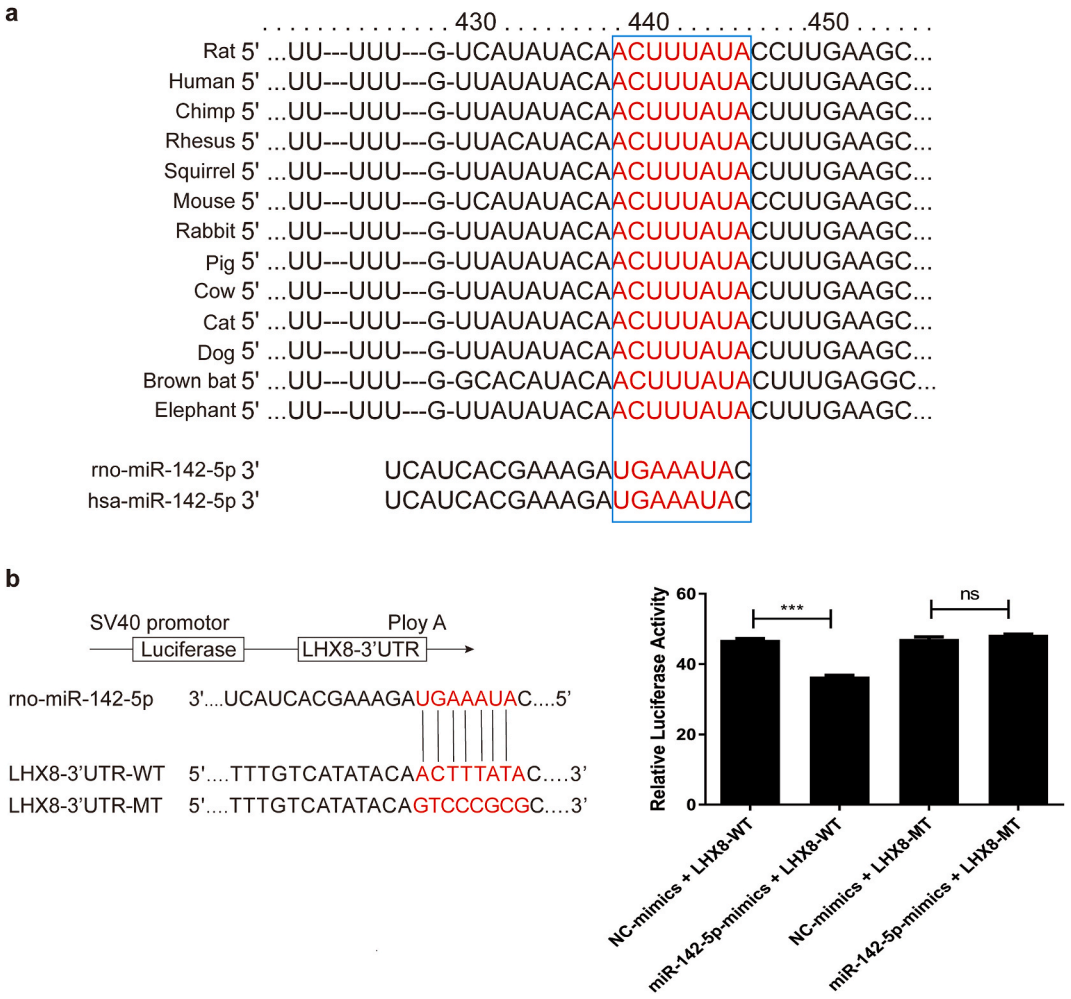

Fig. 5. Lhx8 directly binds to miR-142-5p. a. Different species have the same seed sequence with miR-142-5p; b. Dual luciferase assay verified that Lhx8 directly bound to miR-142-5p.

differentiation was induced in the miR-142-5p mimics-transfected cells and the status of osteogenic differentiation was measured on day 7. miR-142-5p mimics inhibited the expression of the target gene, *Lhx8*, and the osteogenic differentiation-related genes *OPN* and *Runx2*. Additionally, the protein expression levels of Lhx8, OCN, and OPN were downregulated (Fig. 6d and e, Fig. S8).

3.5. Potential competing endogenous RNAs (ceRNA) regulatory network

To elucidate the upstream mechanisms of miR-142-5p/Lhx8 regulation of BMSCs osteogenic differentiation, we analyzed long non-coding RNA (lncRNA) data acquired via RNA sequencing and obtained 3173 lncRNAs. Additionally, 189 differentially expressed lncRNAs, including 131 upregulated lncRNAs and 58 downregulated lncRNA, were identified between both groups based on the following requirements: $|\log 2\ FC| > 2$ and $p.adjust < 0.05$ (Fig. S3). Furthermore, the significantly downregulated lncRNAs with potential competitive binding to miR-142-3p were analyzed using Miranda software version 3.3a. Consequently, four lncRNAs, including LOC120094326, LOC120093052, LOC120097141, and LOC120097383, which may potentially form a ceRNA regulatory network with the miR-142-5p/Lhx8 were identified. The expression levels of lncRNA LOC120094326, LOC120093052, LOC120097141, and LOC120097383 were detected by RT-PCR. The results showed that the four lncRNAs were downregulated in the OVX group. Among them, LOC120094326, LOC120093052, and LOC120097141 were all significantly downregulated (Fig. S3). This result provides a theoretical basis for the next step in our research.

4. Discussion

OP has become a global public health issue, and osteoporotic fractures, with a high incidence rate, and is strongly associated with a high mortality rate [26]. BMSCs are the main source of osteoblasts. Therefore, maintaining their osteogenic differentiation ability at a

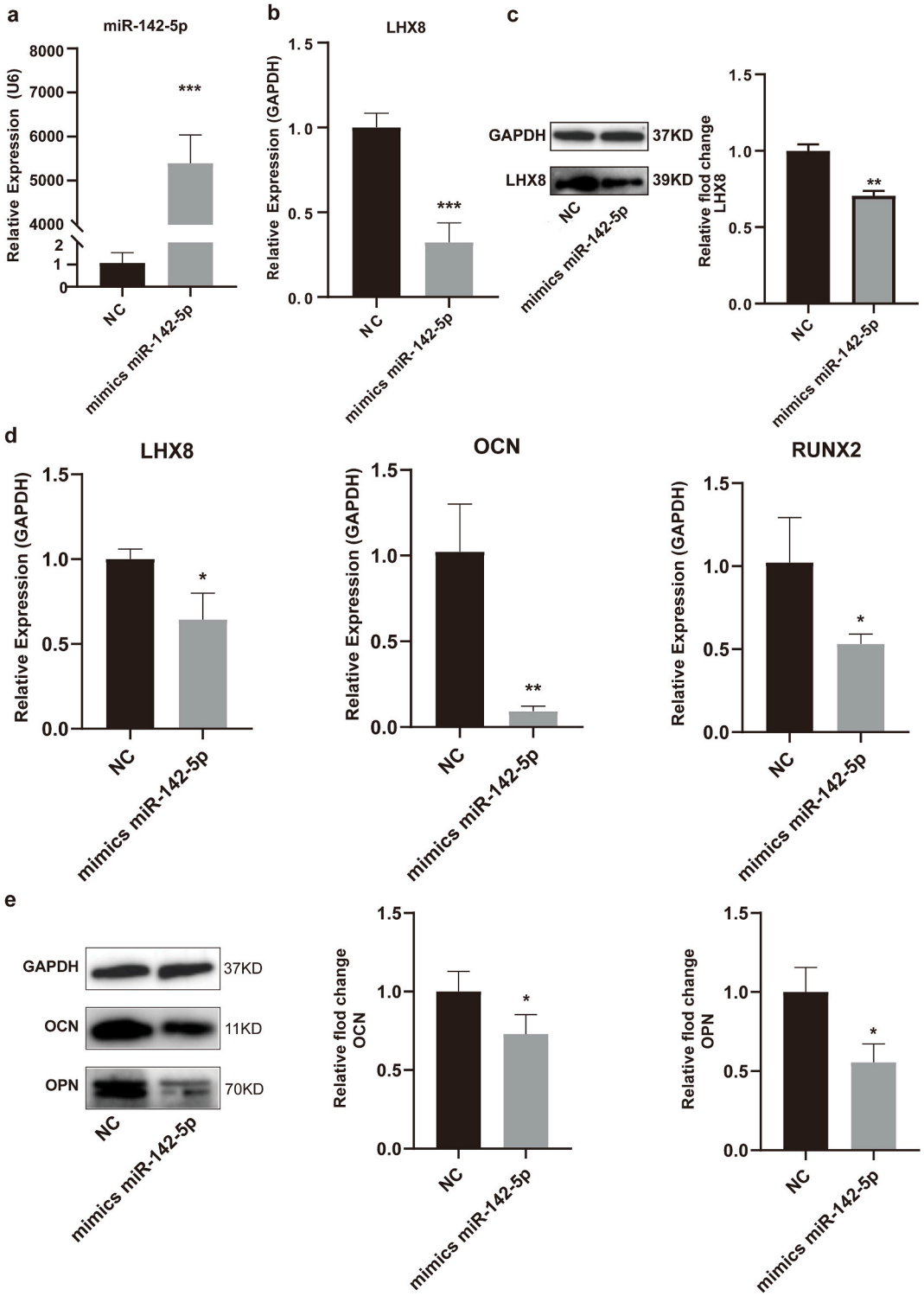

Fig. 6. The interaction between miR-142-5p and Lhx8 inhibits osteogenic differentiation. a. miR-142-5p expression was upregulated after transfection with miR-142-5p mimics; b. *Lhx8* gene expression was downregulated after transfection with miR-142-5p mimics. c. Lhx8 protein expression was downregulated after transfection with miR-142-5p mimics. d. The expression levels of *Lhx8*, *OCN*, and *RUNX2* genes were significantly downregulated miR-142-5p mimic-transfected cells after 7 days of osteogenic differentiation; e. The expression of osteogenic marker proteins OCN and OPN was downregulated in miR-142-5p mimic-transfected cells after 7 days of osteogenic differentiation.

normal level is crucial for regulating bone formation in the body, while the disruption of this process can lead to conditions, such as OP [27]. Our results confirmed that Lhx8 was upregulated during BMSCs osteogenic differentiation. However, the expression of the transcription factor was downregulated in OVX rats, suggesting that Lhx8 may inhibit OP occurrence and progression. Additionally, miRNA-seq of BMSCs from the rats revealed that 34 miRNAs were significantly differentially expressed in the OVX vs sham group, including 17 upregulated and seven downregulated miRNAs. This result indicated the existence of interactions between miR-142-5p and Lhx8 and a potential mechanism of BMSC osteogenic differentiation regulation.

miRNAs play several regulatory roles in cells, including inflammation, oxidative stress and cell growth and differentiation [23]. Certain miRNAs exert promotive effects on OP progression. Previous studies have shown that miR-1297 directly targets Wnt5A and inhibits the osteogenic differentiation of human BMSCs [28]. Additionally, miR-374b-5p directly targets Wnt family member 3 (Wnt3) and Runx2, and negatively regulates the osteogenic differentiation of osteoblasts as well as bone formation [29]. However, some miRNAs can inhibit OP progression. For example, miR-124 promotes osteoblast proliferation and differentiation via the BMP/TGF-β signalling pathway [30]. Additionally, miRNA-291a-3p also directly inhibits DKK1 mRNA and protein expression levels, activates the Wnt/β-catenin signalling pathway, and promotes BMSCs osteogenic differentiation [31]. Moreover, miR-141 overexpression can inhibit mandibular OP in OVR rats by activating the Wnt/β-catenin signalling pathway [32].

miR-142-5p is associated with the occurrence of various diseases and can be used as a target for disease diagnosis. For example, miR-142-5p expression in the tumour microenvironment may serve as a target for diagnosis and treatment [33]. In chronic inflammation, miR-142-5p is capable of regulating macrophage-promoted tissue fibrosis, leading to the occurrence of many end-stage chronic inflammatory diseases [34]. Further, miR-142-5p is downregulated in osteoarthritis and it can directly act on CXCR4 to inhibit chondrocyte apoptosis, thereby alleviating osteoarthritis progression [35]. However, miR-142-5p can also directly target PTEN, which promotes the differentiation of bone marrow-derived macrophages into osteoclasts, thereby promoting osteoclast genesis [36]. Teng et al. showed that miR-142-5p inhibits BMSC migration by suppressing VCAM-1 expression [37]. In the present study, miR-142-5p was significantly upregulated in OP and participated in the negative regulation of the osteogenic differentiation of BMSCs. miR-142-5p sequences and their interaction sites with Lhx8 on the 3'-UTR are highly conserved across different species, indicating that this regulatory relationship may possess widespread applicability. Overall, these results indicate that miR-142-5p is associated with OP progression, making it a potential diagnostic target for OP. Compared to traditional osteoporosis marker proteins, miRNAs are more stable and less influenced by the patient's clinical characteristics [38]. Thus, miR-142-5p is a promising osteoporosis-related biomarker that can compensate for the lack of traditional biomarkers.

ceRNAs, transcripts that can competitively bind RNA [39], include lncRNAs, which can competitively bind miRNAs [40]. The entire regulatory network in which ceRNAs participate is known as the ceRNA regulatory network, and the associated ceRNA network, in which miRNAs play a central regulatory role usually includes lncRNA-miRNA-mRNA. Additionally, the transcription level of the mRNAs regulated by miRNAs increases when miRNAs are competitively bound by ceRNAs, such as lncRNAs. Further, miRNAs and lncRNAs in ceRNA regulatory networks have been shown to function as epigenetic regulatory factors, which play an important role in controlling gene expression and altering various biological processes, including bone metabolism [41]. Moreover, lncRNAs play a key role in OP regulation. For instance, lncRNA-H19 regulates the expression of Angpt1, thus promotes the osteogenic differentiation of mouse BMSCs [42]. In the present study, we confirmed the involvement of miR-142-5p in the regulation of BMSC osteogenic differentiation, and predicted the lncRNAs that interacted with miR-142-5p. This suggests the potential functions of the interacting lncRNAs in BMSCs osteogenic differentiation and OP regulation. Based on these findings, we speculated that the lncRNAs, LOC120094326, LOC120093052 and LOC120097141 may sponge miR-142-5p. Overall, we elucidated the potential ceRNA regulatory network involved in OP regulation, which may serve as basis for future studies on OP.

Author contribution statement

Yongjun Du: Conceived and designed the experiments; Performed the experiments; Analyzed and interpreted the data; Wrote the paper.

Hui Zhong: Conceived and designed the experiments; Performed the experiments.

Chen Yu, Yueyi Yao: Analyzed and interpreted the data.

Yan Lv: Conceived and designed the experiments; Wrote the paper.

Zhi Peng: Wrote the paper.

Sheng Lu: Conceived and designed the experiments.

1 - Conceived and designed the experiments.

2 - Performed the experiments.

3 - Analyzed and interpreted the data.

4 - Contributed reagents, materials, analysis tools or data.

5 - Wrote the paper.

Funding statement

Sheng Lu was supported by Department of Science and Technology of Yunnan Province of China {202001AY070001-172}, Clinical Medical Centre of Spine and Spinal Cord Diseases of Yunnan Province {zx2022000101}, National Natural Science Foundation of China {81960268, 82172442}.

Yueyi Yao was supported by Department of Science and Technology of Yunnan Province of China {202001AY070001-174}.

Data availability statement

Data included in article/supp. material/referenced in article.

Declaration of competing interest

The authors declare that they have no known competing financial interests or personal relationships that could have appeared to influence the work reported in this paper.

Appendix A. Supplementary data

Supplementary data to this article can be found online at https://doi.org/10.1016/j.heliyon.2023.e19878.

References

[1] H.K. Genant, C. Cooper, G. Poor, et al., Interim report and recommendations of the World health organization task-force for osteoporosis, Osteoporos. Int. 10 (4) (1999) 259–264, https://doi.org/10.1007/s001980050224.
[2] I.R. Reid, A broader strategy for osteoporosis interventions, Nat. Rev. Endocrinol. 16 (6) (2020) 333–339, https://doi.org/10.1038/s41574-020-0339-7.
[3] S. Khosla, L.C. Hofbauer, Osteoporosis treatment: recent developments and ongoing challenges, Lancet Diabetes Endocrinol. 5 (11) (2017) 898–907, https://doi.org/10.1016/s2213-8587(17)30188-2.
[4] W. Cao, W. Lin, H. Cai, et al., Dynamic mechanical loading facilitated chondrogenic differentiation of rabbit BMSCs in collagen scaffolds, Regenerative biomaterials 6 (2) (2019) 99–106, https://doi.org/10.1093/rb/rbz005.
[5] J. Kong, L.P. Wan, Z.M. Liu, S.T. Gao, MiR-1301 promotes adipogenic and osteogenic differentiation of BMSCs by targeting Satb2, Eur. Rev. Med. Pharmacol. Sci. 24 (7) (2020) 3501–3508, https://doi.org/10.26355/eurrev_202004_20809.
[6] F. Yu, F. Wu, F. Li, et al., Wnt7b-induced Sox11 functions enhance self-renewal and osteogenic commitment of bone marrow mesenchymal stem cells, Stem cells (Dayton, Ohio) 38 (8) (2020) 1020–1033, https://doi.org/10.1002/stem.3192.
[7] J.Q. Liang, F. Lu, B. Gan, et al., Low-dose tubacin promotes BMSCs proliferation and morphological changes through the ERK pathway, Am. J. Tourism Res. 11 (3) (2019) 1446–1459.
[8] R. Xu, X. Shen, Y. Si, et al., MicroRNA-31a-5p from aging BMSCs links bone formation and resorption in the aged bone marrow microenvironment, Aging Cell 17 (4) (2018), e12794, https://doi.org/10.1111/acel.12794.
[9] Z.W. Luo, F.X. Li, Y.W. Liu, et al., Aptamer-functionalized exosomes from bone marrow stromal cells target bone to promote bone regeneration, Nanoscale 11 (43) (2019) 20884–20892, https://doi.org/10.1039/c9nr02791b.
[10] P. Zhang, H. Zhang, J. Lin, et al., Insulin impedes osteogenesis of BMSCs by inhibiting autophagy and promoting premature senescence via the TGF-β1 pathway, Aging 12 (3) (2020) 2084–2100, https://doi.org/10.18632/aging.102723.
[11] L. Lin, H. Lin, S. Bai, L. Zheng, X. Zhang, Bone marrow mesenchymal stem cells (BMSCs) improved functional recovery of spinal cord injury partly by promoting axonal regeneration, Neurochem. Int. 115 (2018) 80–84, https://doi.org/10.1016/j.neuint.2018.02.007.
[12] J. Zhang, Z. Feng, J. Wei, et al., Repair of critical-sized mandible defects in aged rat using hypoxia preconditioned BMSCs with up-regulation of hif-1α, Int. J. Biol. Sci. 14 (4) (2018) 449–460, https://doi.org/10.7150/ijbs.24158.
[13] G.Z. Ning, W.Y. Song, H. Xu, et al., Bone marrow mesenchymal stem cells stimulated with low-intensity pulsed ultrasound: better choice of transplantation treatment for spinal cord injury: treatment for SCI by LIPUS-BMSCs transplantation, CNS Neurosci. Ther. 25 (4) (2019) 496–508, https://doi.org/10.1111/cns.13071.
[14] R. Xu, G. Shi, L. Xu, et al., Simvastatin improves oral implant osseointegration via enhanced autophagy and osteogenesis of BMSCs and inhibited osteoclast activity, Journal of tissue engineering and regenerative medicine 12 (5) (2018) 1209–1219, https://doi.org/10.1002/term.2652.
[15] C. Zhou, G. Yang, M. Chen, et al., Lhx8 mediated Wnt and TGFβ pathways in tooth development and regeneration, Biomaterials 63 (2015) 35–46, https://doi.org/10.1016/j.biomaterials.2015.06.004.
[16] C. Zhou, D. Chen, J. Ren, et al., FGF8 and BMP2 mediated dynamic regulation of dental mesenchyme proliferation and differentiation via Lhx8/Suv39h1 complex, J. Cell Mol. Med. 25 (6) (2021) 3051–3062, https://doi.org/10.1111/jcmm.16351.
[17] J.Y. Kim, P.H. Choung, USP1 inhibitor ML323 enhances osteogenic potential of human dental pulp stem cells, Biochem. Biophys. Res. Commun. 530 (2) (2020) 418–424, https://doi.org/10.1016/j.bbrc.2020.05.095.
[18] W. Wang, D. Huang, J. Ren, et al., Optogenetic control of mesenchymal cell fate towards precise bone regeneration, Theranostics 9 (26) (2019) 8196–8205, https://doi.org/10.7150/thno.36455.
[19] D. Huang, R. Li, J. Ren, H. Luo, W. Wang, C. Zhou, Temporal induction of Lhx8 by optogenetic control system for efficient bone regeneration, Stem Cell Res. Ther. 12 (1) (2021) 339, https://doi.org/10.1186/s13287-021-02412-8.
[20] L.A. Yates, C.J. Norbury, R.J. Gilbert, The long and short of microRNA, Cell 153 (3) (2013) 516–519, https://doi.org/10.1016/j.cell.2013.04.003.
[21] H. Li, J. Fan, L. Fan, et al., MiRNA-10b reciprocally stimulates osteogenesis and inhibits adipogenesis partly through the TGF-β/SMAD2 signaling pathway, Aging and disease 9 (6) (2018) 1058–1073, https://doi.org/10.14336/ad.2018.0214.
[22] Z. Li, W. Zhang, Y. Huang, MiRNA-133a is involved in the regulation of postmenopausal osteoporosis through promoting osteoclast differentiation, Acta biochimica et biophysica Sinica 50 (3) (2018) 273–280, https://doi.org/10.1093/abbs/gmy006.
[23] Q. Feng, S. Zheng, J. Zheng, The emerging role of microRNAs in bone remodeling and its therapeutic implications for osteoporosis, Biosci. Rep. 38 (3) (2018), https://doi.org/10.1042/bsr20180453.
[24] D. Bellavia, A. De Luca, V. Carina, et al., Deregulated miRNAs in bone health: epigenetic roles in osteoporosis, Bone 122 (2019) 52–75, https://doi.org/10.1016/j.bone.2019.02.013.
[25] S. Huang, V. Leung, S. Peng, et al., Developmental definition of MSCs: new insights into pending questions, Cell Reprogram 13 (6) (2011) 465–472, https://doi.org/10.1089/cell.2011.0045.
[26] P.R. Ebeling, H.H. Nguyen, J. Aleksova, A.J. Vincent, P. Wong, F. Milat, Secondary osteoporosis, Endocr. Rev. 43 (2) (2022) 240–313, https://doi.org/10.1210/endrev/bnab028.
[27] F. Deschaseaux, C. Pontikoglou, L. Sensébé, Bone regeneration: the stem/progenitor cells point of view, J. Cell Mol. Med. 14 (1–2) (2010) 103–115, https://doi.org/10.1111/j.1582-4934.2009.00878.x.
[28] Q. Wang, C.H. Wang, Y. Meng, microRNA-1297 promotes the progression of osteoporosis through regulation of osteogenesis of bone marrow mesenchymal stem cells by targeting WNT5A, Eur. Rev. Med. Pharmacol. Sci. 23 (11) (2019) 4541–4550, https://doi.org/10.26355/eurrev_201906_18029.
[29] Y. Xu, S. Zhang, D. Fu, D. Lu, Circulating miR-374b-5p negatively regulates osteoblast differentiation in the progression of osteoporosis via targeting Wnt3 AND Runx2, J. Biol. Regul. Homeost. Agents 34 (2) (2020) 345–355, https://doi.org/10.23812/19-507-a-9.

[30] X. Xu, L. Zhu, MiR-124 promotes proliferation and differentiation of osteoblasts via BMP/TGF-β signaling pathway, Minerva Endocrinol. 45 (2) (2020) 156–158, https://doi.org/10.23736/s0391-1977.19.03079-7.
[31] Z.H. Li, H. Hu, X.Y. Zhang, et al., MiR-291a-3p regulates the BMSCs differentiation via targeting DKK1 in dexamethasone-induced osteoporosis, The Kaohsiung journal of medical sciences 36 (1) (2020) 35–42, https://doi.org/10.1002/kjm2.12134.
[32] T.J. Liu, J.L. Guo, Overexpression of microRNA-141 inhibits osteoporosis in the jawbones of ovariectomized rats by regulating the Wnt/β-catenin pathway, Arch. Oral Biol. 113 (2020), 104713, https://doi.org/10.1016/j.archoralbio.2020.104713.
[33] C. Zhou, Y. Zhang, R. Yan, et al., Exosome-derived miR-142-5p remodels lymphatic vessels and induces Ido to promote immune privilege in the tumour microenvironment, Cell Death Differ. 28 (2) (2021) 715–729, https://doi.org/10.1038/s41418-020-00618-6.
[34] S. Su, Q. Zhao, C. He, et al., miR-142-5p and miR-130a-3p are regulated by IL-4 and IL-13 and control profibrogenic macrophage program, Nat. Commun. 6 (2015) 8523, https://doi.org/10.1038/ncomms9523.
[35] Y. Xiang, Y. Li, L. Yang, Y. He, D. Jia, X. Hu, miR-142-5p as a CXCR4-targeted MicroRNA attenuates SDF-1-induced chondrocyte apoptosis and cartilage degradation via inactivating MAPK signaling pathway, Biochem Res Int 2020 (2020), 4508108, https://doi.org/10.1155/2020/4508108.
[36] Z. Lou, Z. Peng, B. Wang, X. Li, X. Li, X. Zhang, miR-142-5p promotes the osteoclast differentiation of bone marrow-derived macrophages via PTEN/PI3K/AKT/FoxO1 pathway, J Bone Miner Metab 37 (5) (2019) 815–824, https://doi.org/10.1007/s00774-019-00997-y.
[37] Z. Teng, X. Xie, Y. Zhu, et al., miR-142-5p in bone marrow-derived mesenchymal stem cells promotes osteoporosis involving targeting adhesion molecule VCAM-1 and inhibiting cell migration, BioMed Res. Int. 2018 (2018), 3274641, https://doi.org/10.1155/2018/3274641.
[38] W. Lu, Q. Wang, Y. Xue, et al., Identification of potential osteoporosis miRNA biomarkers using bioinformatics approaches, Comput. Math. Methods Med. 2021 (2021), 3562942, https://doi.org/10.1155/2021/3562942.
[39] L. Salmena, L. Poliseno, Y. Tay, L. Kats, P.P. Pandolfi, A ceRNA hypothesis: the Rosetta Stone of a hidden RNA language? Cell 146 (3) (2011) 353–358, https://doi.org/10.1016/j.cell.2011.07.014.
[40] X. Wu, Z. Sui, H. Zhang, Y. Wang, Z. Yu, Integrated analysis of lncRNA-mediated ceRNA network in lung adenocarcinoma, Front. Oncol. 10 (2020), 554759, https://doi.org/10.3389/fonc.2020.554759.
[41] Y. Yang, W. Yujiao, W. Fang, et al., The roles of miRNA, lncRNA and circRNA in the development of osteoporosis, Biol. Res. 53 (1) (2020) 40, https://doi.org/10.1186/s40659-020-00309-z.
[42] J. Behera, A. Kumar, M.J. Voor, N. Tyagi, Exosomal lncRNA-H19 promotes osteogenesis and angiogenesis through mediating Angpt1/Tie2-NO signaling in CBS-heterozygous mice, Theranostics 11 (16) (2021) 7715–7734, https://doi.org/10.7150/thno.58410.